International Journal of Fluid Machinery and Systems
Vol. 8, No. 2, April-June 2015

DOI: http://dx.doi.org/10.5293/IJFMS.2015.8.2.094
ISSN (Online): 1882-9554

Original Paper

Numerical studies on cavitation behavior in impeller of centrifugal pump with different blade profiles

Pengfei Song[1], Yongxue Zhang[1], Cong Xu[1], Xin Zhou[1] and Jinya Zhang[1]

[1] Mechanical and Transportation Engineering, China University of Petroleum(Beijing), Beijing102249, PR China, spf0322@126.com

Abstract

To investigate the influence of blade profiles on cavitation behavior in impeller of centrifugal pump, a centrifugal pump with five different blade profiles impellers are studied numerically. The impellers with five different blade profiles (single arc, double arcs, triple arcs, logarithmic spiral and linear -variable angle spiral) were designed by the in-house hydraulic design code using geometric parameters of IS 150-125-125 centrifugal pump. The experiments of the centrifugal pump have been conducted to verify numerical simulation model. The numerical results show that the blade profile lines has a weak effect on cavitation inception near blade inlet edge position, however it has the key effect on the development of sheet cavitation in impeller, and also influences the distribution of sheet cavitation in impeller channels. A slight changing of blade setting angle will induce significant difference of cavitation in impeller. The sharp changing of impeller blade setting angle causes obvious cavitation region separation near the impeller inlet close to blade suction surface and much more flow loss. The centrifugal pump with blade profile of setting angle gently changing (logarithmic spiral) has the super cavitation performance, which means smaller critical cavitation number and lower vapor cavity volume fraction at the same conditions.

Keywords: Centrifugal pump, Blade profile, Cavitation behavior, Numerical simulation.

1. Introduction

Cavitation in impeller of centrifugal pump appears mainly nearby impeller inlet and blade suction surface, which lies in the hydraulic losses nearby impeller inlet, including friction loss, incidence loss and blade profile losses. All these types of loss are associated with impeller and blade profile geometric parameters. Especial for the later, it not only affects cavitation inception as with impeller parameters, but also has effect on the development of cavitation and cavity gathering at the blade suction surface.

There are many studies on blade profile design and its effect on flow field in fluid machinery had been completed at home and abroad. Currently, the common used profile lines of cylindrical blade include involute, logarithmic spiral and arc line including single arc line, double arc line and three arc line. Herbich J B [1] has conducted experiment of circular arc blades shows that the efficiency of log spiral blade was highest. Cooper P [2] and Hackworth M [3] proposed that an appropriate blade profile can effectively improve cavitation performance of impeller in the patent of anti-cavitation impeller design. JP Franc [4], Katz J [5] and Franc J P [6] have studied the relationship between cavitation and boundary layer separation of stationary airfoil surface. The result shows that a low pressure zone has been formed behind the point of boundary layer separation which induces cavitation concomitantly. W R [7] and Fogarty [8] have performed some studies on the separation of boundary layer and potential flow near rotating blade using incompressibility and compressibility fluid respectively. The main impacts on rotating arc blade are profile line and the inlet angle. At the same time, rotating blade is better than a stationary airfoil on suppressing boundary layer separation. Dumitrescu H [9] have studied the bubble separation of the leading edge of rotating blades, and it proposed that except for Reynolds number, the blade profile and low pressure zone also affect the separation of leading edge. Trigg M A [10] optimized arc blade profile by adopting genetic algorithm, and the result showed that the hydraulic efficiency of modified impeller with optimized blade profile increased by 10% ~ 20%.

In summary, current research on the relationship between blades surface flow characteristics and cavitation characteristics is mainly static cascade. For the study of rotor blades, since cavitation flow field generated by rotating blades is very complex, which leads to the theoretical or experimental studies existing difficulties. There are few studies on relationship between different blade surface flow characteristics and cavitation performance, which are mostly against the blade inlet conditions such as blade inlet setting angle and inlet edge geometric parameters [14-16]. In addition to the blade inlet conditions, blade profile is an important factor affecting the cavitation performance of rotating blades. Blade inlet conditions affected cavitation inception at the blade entrance, and blade profile affected the development of cavitation. The degree of cavitation development directly affects fluid mechanical to run high efficiently, stably.

Received April 27 2015; accepted for publication June 8 2015: Review conducted by Zhang Yang-jun. (Paper number O105024C)
Corresponding author: Pengfei Song, spf0322@126.com

In this paper, using the basic geometric parameters of IS 150-125-125 centrifugal pump, we complete the hydraulic design of impeller with five different blade profiles (single arc, double arcs, triple arcs, logarithmic spiral and linear -variable angle spiral) through the in-house hydraulic design code. The cavitation flow in these five different impellers and the centrifugal pump impeller were calculated by ANSYS-Fluent with the Zwart-Gerber-Belamri cavitation model. A test rig was set up to conduct the cavitation performance tests of the centrifugal pump to verify the numerical simulation. The effect of different blade profiles on cavitation performance of centrifugal pump, including head drop performance curves, critical cavitation number and cavitation flow field was proposed. Moreover, the relationship between surface flow characteristics of the rotating blades and the development of cavitation is also studied according to the numerical simulation results.

2. Mathematical model of numerical simulation

2.1 **Continuity equation and momentum equation**

Based on the homogeneous multiphase transport equation model, all phases share the same velocity, and the governing mixture equations for continuity and momentum and the vapor phase volume fraction of transport equation respectively are [17]:

$$\frac{\partial \rho_m}{\partial t}+\nabla\cdot\left(\rho_m\vec{u}_m\right)=0 \tag{1}$$

$$\frac{\partial \rho_m\vec{u}_m}{\partial t}+\nabla\cdot\left(\rho_m\vec{u}_m\vec{u}_m\right)=-\nabla p+\nabla\cdot\left[\left(\mu_m+\mu_t\right)\times\nabla\vec{u}_m\right]+\frac{1}{3}\nabla\left[\left(\mu_m+\mu_t\right)\nabla\cdot\vec{u}_m\right] \tag{2}$$

$$\frac{\partial}{\partial t}\left(\rho_v\alpha_v\right)+\nabla\cdot\left(\rho_v\vec{u}_v\alpha_v\right)=R \tag{3}$$

Where ρ_m and ρ_v are the mixture density and vapor phase density, kg/m3; t is the time, s; $\vec{u}_m$ and $\vec{u}_v$ are the mass average velocity and the vapor phase velocity, m/s; μ_m and μ_t are the mixture dynamic viscosity and the turbulence viscosity, kg/(m·s); P is the pressure of flow field, Pa; ρ_m, $\vec{u}_m$ and μ_m are the weighted average of liquid phase and vapor phase which as follows:

$$\rho_m=\rho_v\alpha_v+\rho_l\left(1-\alpha_v\right) \tag{4}$$

$$\vec{u}_m=\vec{u}_v\alpha_v+\vec{u}_l\left(1-\alpha_v\right) \tag{5}$$

$$\mu=\mu_v\alpha_v+\mu_l\left(1-\alpha_v\right) \tag{6}$$

Where $\vec{u}_v$ and $\vec{u}_l$ are the velocity of vapour phase and liquid phase, m/s; μ_v and μ_l are the dynamic viscosity of vapor phase and liquid phase, Pa·s; ρ_l is the liquid phase density, kg/m3; α_v is the vapor phase volume fraction.

The interphase mass transfer rate R is:

$$R=R_e-R_c \tag{7}$$

Where the source terms R_e and R_c denotes vapour generation (evaporation) and condensation rates.

2.2 Cavitation bubble dynamic equation

Assuming that all the bubbles in a system have the same size, Zwart-Gerber-Belamri cavitation model [18-19] is that all bubbles in system share the same radius, the interphase mass transfer rate *R* is:

$$R=F\frac{3\alpha_v\rho_v}{R_B}\sqrt{\frac{2}{3}\frac{\left|p_B-p\right|}{\rho_l}}sign\left(p_B-p\right) \tag{8}$$

Where the source terms p_B and p denote the inside pressure and outside of cavity, Pa; the source term *F* is the empirical calibration coefficient; R_B is the bubble radius, m.

The final form of this cavitation model is as follows:

If $p\le p_v$,

$$R_e=F_{vap}\frac{3\alpha_{nuc}\left(1-\alpha_v\right)\rho_v}{R_B}\sqrt{\frac{2}{3}\frac{p_v-p}{\rho_l}} \tag{9}$$

If $p>p_v$,

$$R_c=F_{cond}\frac{3\alpha_v\rho_v}{R_B}\sqrt{\frac{2}{3}\frac{p-p_v}{\rho_l}} \tag{10}$$

Where α_{nuc} is the nucleation site volume fraction, p and p_v denote the flow field pressure and vapor pressure, Pa, and $p_v=p_B$; the source terms F_{vap} and F_{cond} denote evaporation coefficient and condensation coefficient.

3. Computational domain and mesh

3.1 Impeller model

This paper use the basic geometric parameters and the design flow-lift curve from the IS 150-125-250 centrifugal pump as a known condition, keeping the other parameters unchanged, we complete the hydraulic design of impeller with five different blade profiles including single arc line(model 1), double arc line(model 2), three arc line(model 3), logarithmic spiral(model 4) and setting angle varies linearly spiral (model 5) through the in-house hydraulic design code [20]. Figure 1 shows blade setting angle distribution along the radial direction of 5 impeller blades and figure 2 shows the blade contour line. As shown in Figure 1, blade profile of model 1 only has one arc, and from the initial point to 1/3 blade in radial direction the blade setting angle increases, then decreases. In addition, blade profile of model 2 and 3 have two and three arc respectively, and the change rate of setting angle decreases gradually The relationship between blade setting angle and profile of each point in model 4 and 5 is $\tan\beta = \mathrm{d}r/(r\cdot \mathrm{d}\theta)$, for logarithmic spiral (model 4) $\beta = \text{const}$, for setting angle varies linearly spiral (model 5) $\beta = a\theta + b$, and θ is circumferential angle. To ensure that the design impeller blades match with the pump, the specific design parameters are shown in Table 1. The three-dimensional model of the blades is shown in Figure 3 and its impeller model is shown in Figure 4.

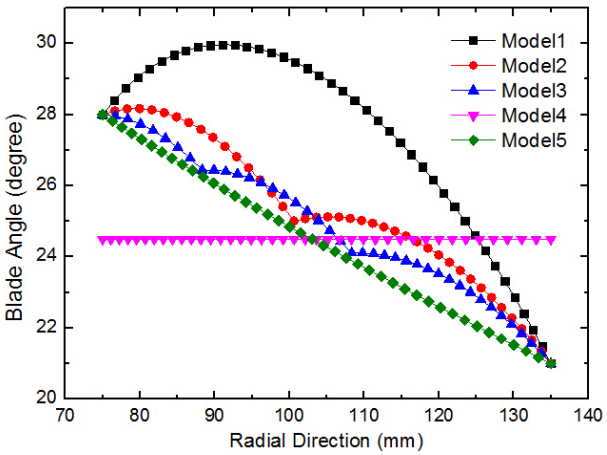

Fig.1 Blade setting angle distribution of five blades

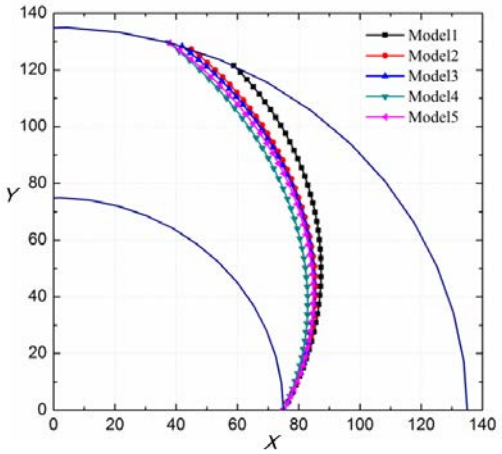

Fig.2 Shape of five blades

Fig.3 Design blade model

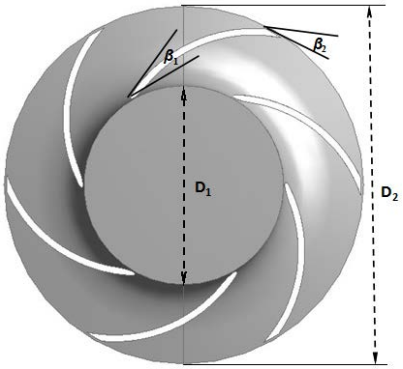

Fig.4 Design impeller model

Tab 1 Design parameters of impeller.

D_1 (mm)	D_2(mm)	B_2(mm)	β_1(°)	β_2(°)	Z	n (rpm)
150	270	30	28	21	6	1450

3.2 Computational fluid dynamics

The numerical simulation is conducted with the framework of the ANSYS-Fluent solver. The homogeneous two-phase mixture model is selected for cavitating computation, and the k-ε turbulence model is mainly used. The computational domain consists of four parts which are inlet extended section, impeller, volute, outlet extended section. Figure 5 shows the grid of 3D pump and partial grid on impeller. Moreover, we also adopt properly refinement of mesh near blade inlet edge and blade surface as shown in figure 5(b). The total number of 1.7 million grids has been founded to be suitable for numerical simulation after the grid independence test being made. The boundary conditions of simulations are set as follows: The inlet of the calculation domain is specified by using the averaged mass flow rate, and the volume fraction of vapor phase is set to zero. At the outlet boundary, an average static pressure is set according to total pressure level at the domain inlet. All solid walls are set as the non-slip wall condition. At the same time, impeller region coupling with other regions adopt mesh motion.

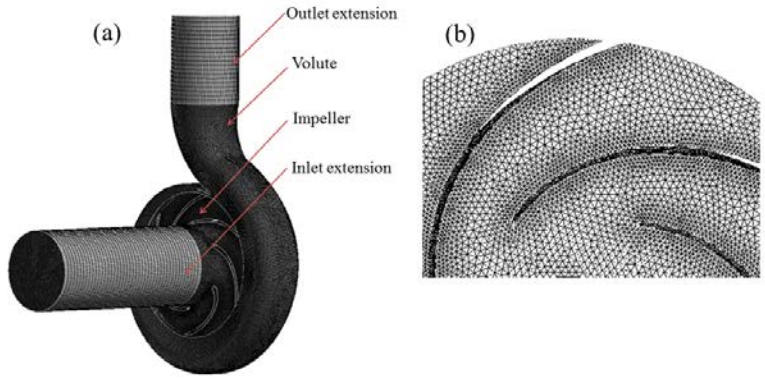

Fig.5 Mesh applied for the calculation. (a) 3D view of pump, (b) partial view of mesh on impeller hub

4 Results and Discussion

Three dimensionless parameters are defined to describe the cavitation flow in centrifugal pump as follows: Cavitation number $\sigma = (p_\infty - p_v)/0.5\rho_l U_2^2$, Head coefficient $\psi = H/(U_2^2/2g)$, Flow coefficient $\varphi = Q/\pi D_2 b_2 U_2$. Where p_∞ is inlet static pressure, Pa; ρ is fluid density, kg/m^3; p_v is vaporization pressure of liquid phase, Pa; H is the head of centrifugal pump, m; U_2 is the peripheral speed of impeller outlet, m/s.

4.1 The reliability verification of numerical simulation

Figure 6 shows the head-drop curves of experiment and simulation at flow coefficient φ=0.103 and φ=0.112. In non-cavitation conditions, numerical simulation has a slight overestimation of head coefficient. Compared to experiment result, the deviations are respectively 0.64% and 2.2% at φ=0.103 and φ=0.112, which mainly due to the leakage loss in pump is not considered in numerical simulation. With decreasing cavitation number, the deviation of head coefficient has a tiny increasing (smaller than 5%). It is because that the interaction of cavitation bubbles and hydraulic loop of cavitation cloud are not considered in simulation. However, the numerical simulation predicts the variation trend of head well.

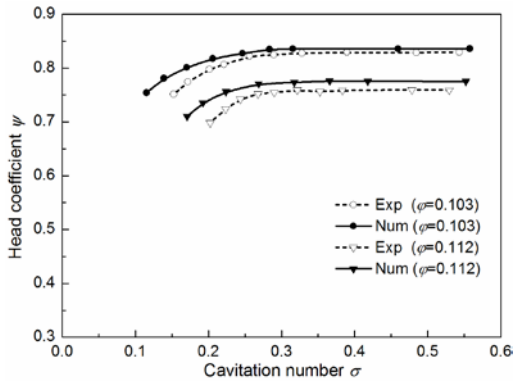

Fig.6 Head-drop curves of experiment and simulation at φ=0.103 and φ=0.112

4.2 Analysis of head drop performance curves

Figure 7 shows the head drop curves of pump in cavitating condition for different models at flow coefficient φ=0.103 conditions. As can be seen from the figure, the changing trend of head drop curves of five models in cavitating condition is consistent, which means the head coefficient firstly keep in constant with the cavitation number decreasing, when the cavitation number decreases to a certain value, the external characteristic curve turns out to have a turning point, and the head coefficient decreased rapidly after the turning point. However, the position of turning points is different, and so does the declined slop of head coefficient. Note that the cavitation number corresponding to the turning point of model 4 is obviously smaller than other models.

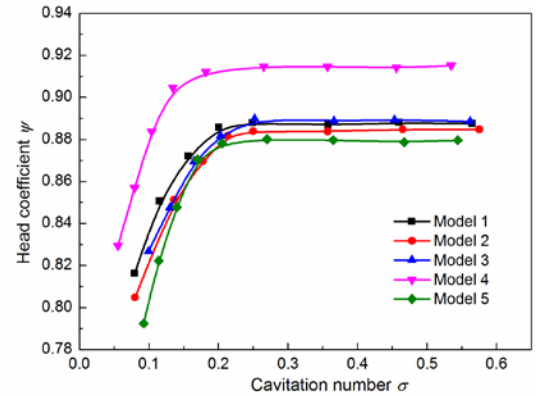

Fig.7 Head drop curves in cavitating condition for different impeller models

Qualitative explanation is not sufficient to characterize the cavitation performance of a centrifugal pump, so it requires quantitative analysis. Currently the critical cavitation number as the head declining by 3% has been used to measure the cavitation performance of pump in industry or academic aspect. Table 2 shows the critical cavitation number of five different impeller blades through numerical simulation. Obviously we can see that critical cavitation number of model 4 is the smallest and model 1 is the biggest. It illustrates that logarithmic spiral as blade profile line has better cavitation performance. Note that the critical cavitation number of Model 1, Model 2, model 3 and model 5 is decreasing in turn, which suggests the more gently blade setting angle varies, the smaller critical cavitation number.

Tab.2 Critical cavitation number of centrifugal pump for different models

	Model 1	Model 2	Model 3	Model 4	Model 5
Critical cavitation number $\sigma_{3\%}$	0.162	0.154	0.149	0.108	0.139

4.3 Analysis of cavitation flow field in impeller

The sheet cavitation in impeller channels and cavity length on blade suction surface can represent the amount of developed cavitation and are appropriate representation of the cavitation bubble growth and cavitation intensity. Figure 8 shows the impeller axial cross section contours of sheet cavitation blocking the impeller channels at flow coefficient φ= 0.103 and cavitation number σ=0.11. From figure 8, the distribution of sheet cavitation in impeller for different model shows that the cavitation area of model 1 is biggest which induces blocking impeller channels seriously, and model 4 is smallest. Note that the cavitation area of other three models has no obvious difference. However, the sheet cavitation near blade suction surface of these three models appears separating form the surface with different extent, which directly causes the sheet cavitation diffusing from suction surfaces to impeller channel, and then leads to serious influence on liquid phase flowing. The analysis of above indicates that the blade profile line has an essential effect on the area of sheet cavitation in impeller, and also influences the distribution of sheet cavitation in impeller channels. For example, the blade profile line adopting logarithmic spiral is conducive to inhibiting the development of cavitation in impeller channels.

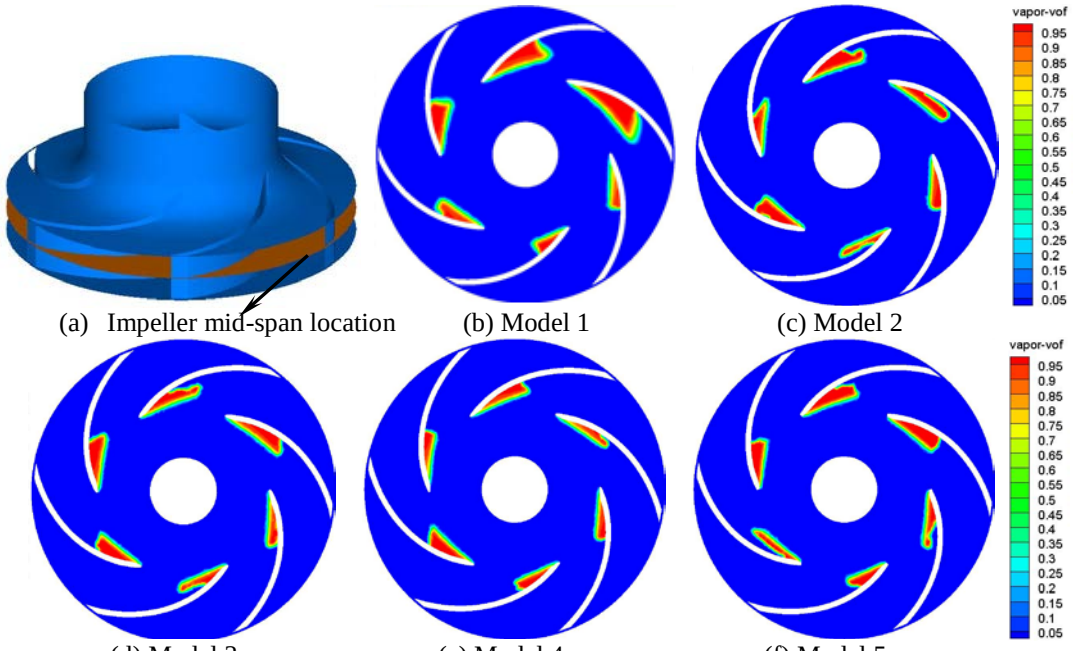

(a) Impeller mid-span location (b) Model 1 (c) Model 2

(d) Model 3 (e) Model 4 (f) Model 5

Fig.8 The vapor cavity distribution in impeller mid-span

Figure 9 shows and the extent of vapor cavity development for the impeller mid-span location at σ=0.11 and σ=0.21. Because the cavitation region near blade suction surface appears separating from the surface at σ=0.11, it cannot be used to quantitatively assess the extent of cavitation on the blade suction surface. Thus, taking the σ=0.21 condition for instance, we conduct quantitative analysis of vapor cavity development on blade suction surface, which has no appearing of cavitation region separating from the surface as shown in figure 8. As can be seen from figure 9, the cavity lengths on the blade suction surface of the five models are different. The length of vapor cavity on the blade suction surface of model 1 is longest, and model 4 is shortest. Compared to model 1, the cavitation length of model 4 approximately decreases by 35%. Moreover, there is also an interesting phenomenon that the vapor cavity volume fraction on blade suction surface reach the maximum near the one-tenth length of blade for five models at σ=0.11 and σ=0.21, and the value of volume fraction at the same position of blade exist tiny differences within one-tenth length of blade. This also illustrates that different blade profiles have a weak effect on cavitation inception near blade leading edge, however, it essentially influences on cavitation development in impeller channels.

With carefully analyzing figure 9(b), we can see that the cavitation length on blade suction surface decreases in turn as the order of model 4, model 5, model 3, model 2 and model 1, which illustrates the gently changing of blade setting angle is conducive to weaken the cavitation intensity in impeller at the same condition. This result is consistent with the analysis result of critical cavitation number for different blade profiles.

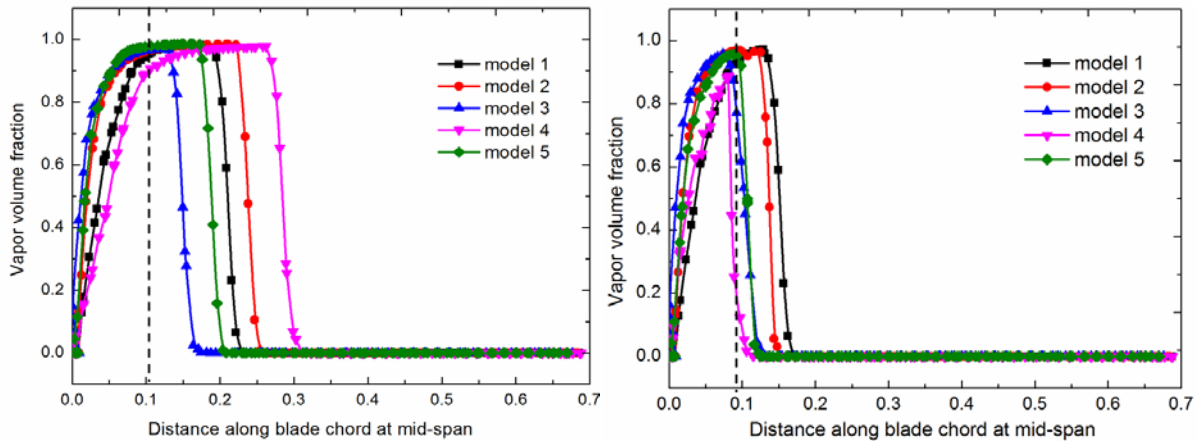

(a) Cavitation number σ=0.11 (b) Cavitation number σ=0.21

Fig.9 Vapor cavity lengths in impeller mid-span

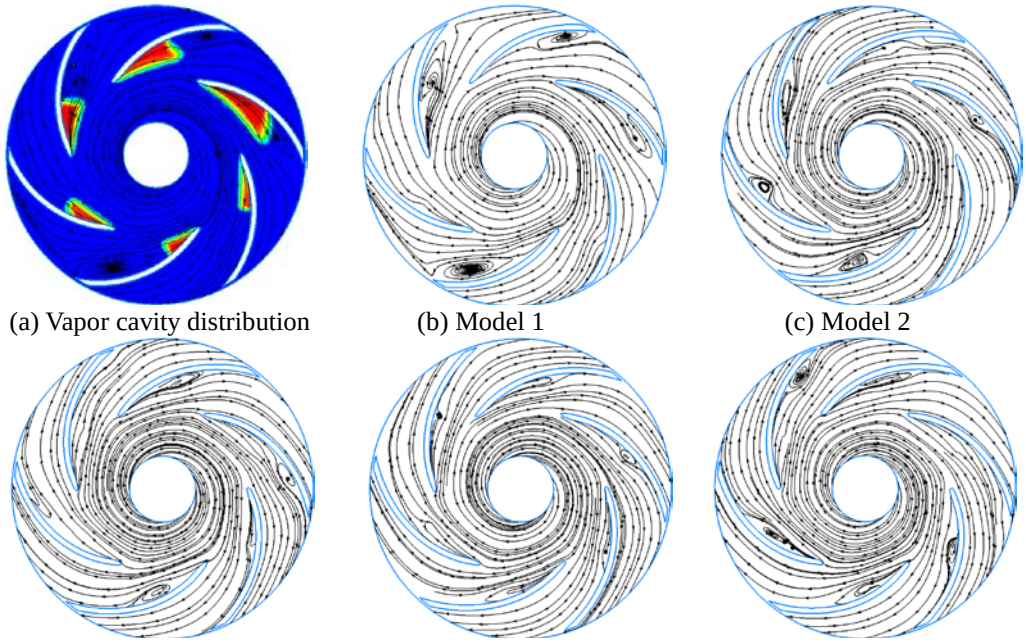

(a) Vapor cavity distribution (b) Model 1 (c) Model 2

(d) Model 3 (e) Model 4 (f) Model 5

Fig.10 Path Line distribution in impeller channel space

Figure 10 shows the streamline distribution of the impeller mid-span location at the flow coefficient φ=0.103 and pump inlet cavitation number σ=0.11 condition. The black lines with arrow in the figure indicate the streamline in figure 10. As we can see from figure 10, the cavitation flow field in impeller of five models exist vortices, which are formed at the trail of cavitation areas. By carefully observing the vortices and streamline of every graph, we can find that all models have several flow vortices in field of cavitation flow. Note that model 4 has fewer and feebler vortices, however, there are some very obvious vortices in other four models, especially model 1. Therefore, it concludes that the development of cavitation has closed relationship with those vortices. The sharp changing of blade setting angle causes cavitation region separating form blade suction surface, and then results in some obvious vortices in impeller channels, which induces the further cavitation developing and much flow losses. In a word, the blade profile line adopting logarithmic spiral is conducive to inhibiting flow separation of blade surface, and then weakening the development of cavitation in impeller.

5 Conclusions

This paper studies the effect of five different blade profiles on cavitation performance of centrifugal pump, including critical cavitation number, head-drop curves and cavitation flow field. According to the research, the following conclusion can be drawn.

The numerical simulation of cavitation in the certain centrifugal pump indicates that the vapor cavity volume fraction on blade suction surface reach the maximum near the one-tenth length of blade for different blade profiles and different cavitation numbers,

and the value of volume fraction at the same position of blade exist tiny differences within one-tenth length of blade. This illustrates that different blade profiles have a weak effect on cavitation inception near blade inlet edge position.

However, the blade profile line has the key effect on the sheet cavitation development in impeller channels. A slight change of blade setting angle will induce significant difference of cavitation in impeller. The sharp changing of impeller blade setting angle causes obvious cavitation region separation near the impeller inlet close to blade suction surface and much more flow loss. The centrifugal pump with blade profile of blade setting angle gently changing (logarithmic spiral) has the super cavitation performance, which means smaller critical cavitation number and lower vapor cavity volume fraction at the same conditions. In addition, the cavitation length on suction surface also approximately decreases by 35%.

Acknowledgments

This work was supported by the National Science Foundation of China (Grant number 51209217) and Science Foundation of China University of Petroleum, Beijing (Grant number 2462015YQ0411)

Nomenclature

η	hydraulic efficiency	D_1	impeller diameter at inlet
β_1	inlet blade angle of impeller	D_2	impeller diameter at outlet
β_2	outlet blade angle of impeller	H	head of pump
Ψ	head coefficient	Z	blade number
φ	flow coefficient	Q	flow rate
$B2$	impeller width at outlet	M	impeller torque
n	rotate speed	U_2	peripheral velocity at impeller outlet
σ	cavitation number	p_∞	inlet static pressure
p_v	vaporization pressure	ρ_l	fluid density

References

[1] Herbich J B. Modifications in Design Improve Dredge Pump Efficiency[R]. LEHIGH UNIV BETHLEHEM PA FRITZ ENGINEERING LAB, 1962.

[2] Cooper P, Sloteman D P. Impeller for centrifugal pumps: U.S. Patent 5,192,193[P]. 1993-3-9.

[3] Hackworth M, Eslinger D, Harrell N R. Impeller for centrifugal pump: U.S. Patent 7,549,837[P]. 2009-6-23.

[4] Franc, Jean-Pierre, and Jean-Marie Michel, eds. Fundamentals of cavitation. Vol. 76. Springer, 2006.202-204.

[5] Katz J. Cavitation phenomena within regions of flow separation[J]. Journal of Fluid Mechanics, 1984, 140(4): 397-436.

[6] Franc J P, Michel J M. Attached cavitation and the boundary layer: experimental investigation and numerical treatment[J]. Journal of Fluid Mechanics, 1985, 154: 63-90.

[7] Sears W R. Potential flow around a rotating cylindrical blade[J]. Journal of the Aeronautical Sciences (Institute of the Aeronautical Sciences), 2012, 17(3).

[8] Fogarty L E. Potential flow around a rotating, advancing cylindrical blade[J]. Journal of the Aeronautical Sciences (Institute of the Aeronautical Sciences), 2012, 17(9).

[9] Dumitrescu H, Cardos V. Analysis of leading-edge separation bubbles on rotating blades[J]. Journal of Aircraft, 2010, 47(5): 1815-1819.

[10] Trigg M A, Tubby G R, Sheard A G. Automatic genetic optimization approach two-dimensional blade profile design for steam turbines[J]. Journal of turbomachinery, 1999, 121(1): 11-17.

[11] Xu Y. The theory study of circular blade profile line[J]. Fluid Machinery, 1990, 08: 007.

[12] Xu Y. The drawing method of cylindrical blade with variable angle spiral[J]. Fluid Machinery, 1989, 7: 006.

[13] Jing Y. Design of Cylindrical Blade with Involute Contour[J]. Transactions of the Chinese Society of Agricultural Machinery, 2003, 34(5): 80-81.

[14] Coutier-Delgosha O, Hofmann M, Stoffel B, et al. Experimental and numerical studies in a centrifugal pump with two-dimensional curved blades in cavitating condition[J]. Journal of Fluids Engineering, 2003, 125(6): 970-978.

[15] Luo X, Zhang Y, Peng J, et al. Impeller inlet geometry effect on performance improvement for centrifugal pumps[J]. Journal of mechanical science and technology, 2008, 22(10): 1971-1976.

[16] Hirschi R, Favre J N, Parkinson E, et al. Centrifugal pump performance drop due to leading edge cavitation: numerical predictions compared with model tests[J]. Journal of fluids engineering, 1998, 120(4): 705-711.

[17] Batchelor G K. An introduction to fluid dynamics[M]. Cambridge university press, 2000.
[18] Zwart P J, Gerber A G, Belamri T. A two-phase flow model for predicting cavitation dynamics[C]//Fifth International Conference on Multiphase Flow, Yokohama, Japan. 2004.
[19] Mejri I, Belamri T, Bakir F, et al. Comparison of computational results obtained from a homogeneous cavitation model with experimental investigations of three inducers[J]. Journal of fluids engineering, 2006, 128(6): 1308-1323.
[20] Zhou X, Zhang Y, Ji Z, et al. The Optimal Hydraulic Design of Centrifugal Impeller Using Genetic Algorithm with BVF[J]. International Journal of Rotating Machinery, 2014.